

Optical counterpart of Foucault pendulum.

A.Yu.Okulov*

Russian Academy of Sciences, 119991, Moscow, Russian Federation.

(Dated: November 26, 2024)

The twin beam vortex interferometer with phase-conjugating mirror is analyzed in rotating reference frame. Circular motion of the interference pattern occurs due to exchange of the angular momenta between photons and interferometer. Using the concept of the *ideal* phase-conjugating mirror it is shown that motion of the helical interference pattern of the interacting vortex photons with topological charge ℓ may be used for the detection of the slow rotations. The higher density of interference fringes may improve the sensitivity by factor containing 2ℓ compared to the conventional Michelson interferometry.

PACS numbers: 42.50.Tx 42.65.Hw 42.50.Lc 04.80.Nn

I. INTRODUCTION

The rotation of the Earth was a one of the most controversial issues of natural philosophy during centuries in transition from Medieval period to Renaissances and afterwards. The invention of Foucault pendulum [1] and mechanical gyro realized by Johann Bohnenberger in 1817 did not stopped these controversies but ignited further studies of the Earth motion stimulated by navigation needs. The necessity to check the hypothesis of the "ether wind" have led to construction of the highly effective optical instruments [2]. Michelson interferometer gave possibility to detect the small displacements and star's dimensions [3]. Sagnac gyro proved to be highly sensitive to phase lag between counterpropagating waves caused by rotation of the reference frame [4]. Nowadays Maxwell electrodynamics and Einstein relativity explain well the Sagnac effect which is in the heart of the widespread rotation sensors, technically implemented as a passive fiber gyroscopes and the active laser gyros [5]. In the LIGO project [6, 7] the Michelson interferometry with ultra long arms and ultra narrow linewidth laser sources have become conventional instrument in the gravitational waves search [8].

In current work we analyze the new principle of the reference frame rotation detection based upon angular Doppler effect for photons [9] and wavetrain dislocations [10] (fig.1). The rotations of optical quanta are different from a classical mechanical top. Compared to classical mechanics the angular momentum projection on given axis \vec{Z} may have only discrete values proportional to the Plank's constant \hbar [11, 12]. The other feature of the optical vortex interferometry is robustness of the vortex beams [13, 14] with respect to the irregularities in optical path [15]. This is due to conservation of the orbital angular momentum (OAM) projection $\mathcal{L}_z = \pm\ell\hbar$ in a free space [18] for the optical vortices [16, 17] with winding number ℓ . On the other hand rotations of the optical el-

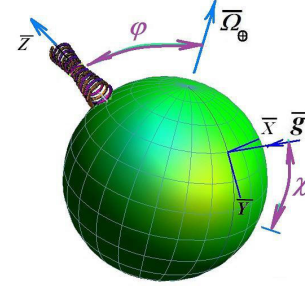


FIG. 1: (Color online) Geometric phase $\alpha(t)$ acquired by Foucault pendulum and vortex interferometer with PCM. For the angle ϕ between ℓ -charged vortex rotation \vec{Z} axis and frame rotation axis $\vec{\Omega}_{\oplus}$ the geometric phase is $\alpha_{pc}(t) = -2\ell|\Omega_{\oplus}|t \cos \phi$ (for $\xi = 0$). Local gravity acceleration \vec{g} indicates location of Foucault pendulum whose swing plane is rotated by Coriolis force to angle $\alpha_F(t) = -|\Omega_{\oplus}|t \sin \chi$. $X, Y, -\vec{g}$ are local coordinates for pendulum, χ is latitude. The angle ϕ is in meridional plane and ξ is out of meridional plane angle (ξ is set to zero hereafter for brevity without loss of rigor).

ements in interferometer affect propagating photons [19]. This gives experimental possibility to detect the angular velocity $\vec{\Omega}_{\oplus}$ of the reference frame with optical vortex interferometer and angular Doppler effect. The key feature of the proposed phase-conjugating vortex interferometer (PCVI) is the usage of wavefront reversing mirror (PCM) [20] which alters direction of the photon's angular momentum [21].

In comparison with previous considerations that use the concept of geometric phases and analogies with Foucault pendulum and Coriolis force experienced by photons [22–28] current approach demonstrates visual similarity of the circular interference pattern rotating due to angular Doppler shift and *seemingly* circular motion of stop points of Foucault pendulum bob (fig.2). In both cases the observable motion is induced via nontrivial angular momentum changes in noninertial reference frame. Noteworthy the exact solutions for angular velocity of rotation exist in explicit form in both cases.

The angular momentum of photons is not changed when observed from reference frames rotating with dif-

*Electronic address: alexey.okulov@gmail.com;
URL: <https://sites.google.com/site/okulovalexey>

ferent angular velocities [29]. But when rotating photons pass the rotating medium the angular momentum does change and the medium experiences recoil [9, 30]. This happens when vortex photons propagate in the interferometer placed upon a surface of the rotating rigid sphere [31] (fig.1). As a result of the such spin-orbital interaction the carrier frequency ω of the vortex photon is shifted as follows:

$$\delta\omega(t) = -\vec{\mathcal{L}}(t) \cdot \vec{\Omega}_{\oplus}/\hbar = -\ell\vec{Z}(t) \cdot \vec{\Omega}_{\oplus}. \quad (1)$$

When interferometer is placed somewhere in equatorial plane with $\chi = 0$ or at the Pole with $\pm\chi = 90^\circ$ (where χ is geographical latitude) $\delta\omega$ is just rotational Doppler shift which has maximal value $\delta\omega = \mp\Omega_{\oplus}\mathcal{L}_z/\hbar$ at $\phi = 0$ and $\delta\omega = 0$ for $\phi = \pi/2$. For arbitrary location of PCVI spin-orbit interaction leads to Coriolis frequency shift of photon $\delta\omega(t) = -\vec{\mathcal{L}}(t) \cdot \vec{\Omega}_{\oplus}/\hbar$. In the same way the conventional Foucault pendulum operates due to the geometric phase $\alpha = -2\pi \sin \chi$ [32] acquired via transport of rotating top along a closed trajectory, where $\phi = \pi/2 - \chi$ is the angle between rotation axis $\vec{\Omega}_{\oplus}$ and angular momentum $\vec{\mathcal{L}}_F(t)$, χ is the geographical latitude (fig.1).

The paper is organized as follows. In section II the geometry of PCVI is described as an extension of the Beth spin angular momentum detection experiment [33], in the section III the interference patterns in both arms of the vortex Michelson interferometer are analyzed taking into account the imperfect coherence γ of the laser source, in the section IV the geometric phase shift $\alpha = \int \delta\omega dt$ is obtained from the space-time symmetries, in the section V the effects of the phase noise of laser source [34] and PCM noise [35] are evaluated taking into account the possibility of quantum noise reduction with topologically charged LG-beams [36], in section VI the results are summarized.

II. CONFIGURATION OF THE VORTEX MICHELSON INTERFEROMETER

Let us begin with the classical experiment on the optical angular momentum measurement performed by Beth in 1936 [33]. The circularly polarized light with angular momentum $\pm\hbar$ per photon had been transmitted through the $\lambda/2$ plate suspended on the quartz wire. Such transparent plates are made from *anisotropic* material (quartz) which changes the angular momentum of the each photon to the opposite one $\mp\hbar$ during passage through the plate. In accordance with the second Newton's law and the angular momentum $\vec{\mathcal{L}}$ conservation the plate experienced the torque $\vec{T} = \Delta\vec{\mathcal{L}}/\Delta t$, where $\Delta\vec{\mathcal{L}}$ is the angular momentum change during time interval Δt . The torque occurs because of the *noncollinearity* of the electric field vector of light \vec{E} and macroscopic polarization $\vec{P}dV$ (dipole moment of the volume dV) inside the birefringent plate. This noncollinearity is manifestation of an anisotropy of the $\lambda/2$ plate which makes

the vector product $\vec{E} \times \vec{P}$ nonzero. The arising torque is $\vec{T} = \epsilon_0 \int (\vec{P} \times \vec{E}) dV \cong 2 \cdot I \cdot \pi D_p^2 / \omega_{f,b}$, where 3D integral is calculated over the plate volume, I is the light intensity, D_p is diameter of plate and $\omega_{f,b}$ are the carrier frequencies of the light waves which travel in the forward (f) or backward(b) direction of Z -axis. Thereby the suspending wire had been twisted and a certain deflection of the plate from the equilibrium position had been detected. In order to enhance the torque Beth reflected the light backwardly by a traditional metallic mirror. The important feature of his setup is an additional $\lambda/4$ plate placed near mirror *to alter spin angular momentum* to double the optical torque via return passage through the suspended $\lambda/2$ plant. Without $\lambda/4$ plate the algebraic sum of torques on the suspended plate would be zero. In fact $\lambda/4$ plate performed the phase-conjugation of reflected wave and the *spin angular momentum* of photons had been reversed.

Our proposal is to replace the traditional mirror by wavefront reversing mirror [37] which alters *orbital angular momentum* (OAM) of photons [21], replace $\lambda/2$ plate by a sequence of the N image altering elements (alike Dove prism) [17] and to use a higher-order optical vortices with angular momentum $\pm\ell\hbar$ per photon [12] instead of circularly polarized light whose AM is just $\pm\hbar$. The possible phase-conjugation mirrors for this purpose might be the photorefractive crystals [38] or the static 3D holograms [39]. The else opportunity is nondegenerate four-wave mixing in an alkali atomic vapors where efficient phase conjugated reflection from 10^5 atoms in thermal cloud had been reported [40]. The other tool for the phase conjugation of the $\pm\ell\hbar$ optical vortices is in multiple reflections from conventional mirrors in the Sagnac loop interferometer [41]. Thus by virtue of the phase conjugating mirror Beth's torsion pendulum setup is transformed into *vortex interferometric* setup realized in Denz group [42] (fig.2). Instead of the altering the *spin* component of photon's angular momentum, the alternation of the *orbital angular momentum* had been realized in this setup with commonly available optical components [43].

The interference pattern between the beamsplitter BS and PCM which arise due to the reversed orbital angular momentum of the backwardly reflected phase conjugated replica $E_b(t, z, r, \theta) = E_f^*(t, z, r, \theta)$ has a nontrivial geometry. In contrast to the speckle patterns composed of vortex-antivortex pairs [44] and the complex regular images generated by vortex arrays[45] this isolated vortex pattern is composed of the 2ℓ mutually embedded helices (fig.2) [46, 47]:

$$|\vec{E}|^2 = |E_f + E_b|^2 \cong I(z, r, \theta, t) \sim [1 + \gamma[2(L_{PCM} - z)] \cdot \cos[(\omega_f - \omega_b)t - (k_f + k_b)z + 2\ell\theta]] \cdot (r/D_0)^{2|\ell|} \exp\left[-\frac{2r^2}{D_0^2(1 + z^2/(k_{(f,b)}^2 D_0^4))}\right], \quad (2)$$

where the cylindrical coordinates (z, r, θ, t) are used, $k_{f,b}$ are the wavenumbers of the E_f and E_b respectively,

$I(z, r, \theta, t)$ is the light intensity distribution of the 2ℓ intertwined helices, $\gamma[2(L_{PCM} - z)]$ is the temporal correlation function of the laser beam which vanishes when $2(L_{PCM} - z) > L_{coh}$, L_{coh} is coherence length of the laser source, L_{PCM} is length of the PCM arm, D_0 is the radius of $LG_{0\ell}$ vortex. Apart from spirality the formula (2) describes *synchronous rotation* of the all 2ℓ helices around the propagation axis z with angular velocity $(\omega_f - \omega_b)/2\ell$ [21]. The rotation appears when the carrier frequencies of the forward E_f and backward waves E_b are different. The electric field envelopes were taken above in the form of Laguerre-Gaussian beams (LG) [21]:

$$E_{(f,b)}(\vec{r}, t) \sim \frac{\exp[-i\omega_{(f,b)}t \pm ik_{(f,b)}z \pm i\ell\theta + i\Theta_{(f,b)}(t)]}{(1+iz/z_R)} \times E_{(f,b)}^0(r/D_0)^{|\ell|} \exp\left[-\frac{r^2}{2D_0^2(1+iz/z_R)}\right], z_R = k_{(f,b)}D_0^2. \quad (3)$$

Alternatively the Bessel beam optical vortices may be considered [48]:

$$E_{(f,b)}(\vec{r}, t) \sim E_{(f,b)}^0 \cdot J_m(\kappa r) \exp[-i\omega_{(f,b)}t \pm ik_{(f,b)}z \pm i\ell\theta + i\Theta_{(f,b)}(t)]. \quad (4)$$

In both cases the random variations of the phases of vortex waves (phase diffusion) $\Theta_{(f,b)}(t)$ are induced by the finite laser linewidth with coherence time $\tau_{coh} = L_{coh}/c$ [54]. Phase diffusion $\Theta_{(f,b)}(t)$ leads to the diminished visibility $\gamma[2(L_{PCM} - z)]$ for nonzero path difference.

We will consider the frequency splitting induced by the angular momentum transfer from photons to *rotating* interferometer or vice versa. Due to OAM exchange photons may acquire the energy from rotating interferometer components or deliver it to interferometer.

III. SPATIAL PATTERNS DUE TO EXCHANGE OF ROTATIONS BETWEEN PHOTONS AND INTERFEROMETER

The mutual exchange of the energy and angular momentum between photons and Mach-Zehnder interferometer had been reported by Dholakia group in 2002 yet [49] where the the interference patterns revolving with Hz-order frequencies were recorded. In essence there is no difference whether a single element rotates say Dove-prism [43] or $\lambda/2$ plate [49] or entire interferometric setup is rotated as a whole. In all these cases the rotational Doppler shift $\delta\omega$ occurs due to the angular momentum exchange between photons and setup. The phase-conjugating mirror will substantially simplify the implementation of such *sub-Hz* rotation sensor because of the self-adjustment property of the PCM [20]. The perfect match of amplitudes and phases of forward and backward waves achieved in the Woerdemann-Alpmann-Denz photorefractive interferometer setup [42] have resulted in a remarkable *two-spot* output pattern obtained

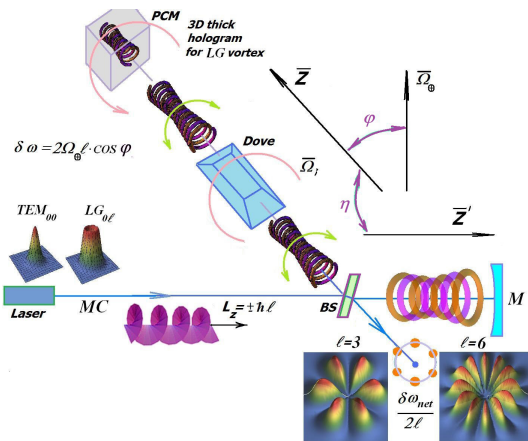


FIG. 2: (Color online) Phase-conjugating vortex interferometer PCVI with topological charge ℓ [42] aligned along the axis \vec{Z} . The azimuthal interference fringes for $\ell = 3$ and for $\ell = 6$ are shown. Single spatial mode TEM_{00} laser output is transformed by mode converter MC in optical vortex with topological charge $\ell = 1, 3, 6, etc.$ The N counter-rotating with respect to each other Dove prisms with angular velocities $\vec{\Omega}_i$ (only one shown) and PC mirror rotating with angular velocity $\vec{\Omega}_\oplus$ alter the photon's angular momentum thereby the angular frequency shift $\delta\omega_{net}$ appears. Angle ϕ is a tilt of \vec{Z} axis to the frame rotation axis $\vec{\Omega}_\oplus$. The angle η between \vec{Z} and \vec{Z}' axes affects interference pattern between "helical" and "toroidal" arms of Michelson PCVI. Response of interferometer reaches maximum when η tends to zero.

by virtue of the beamsplitter BS placed at the entrance of interferometer (fig.2). Two-spot output of this vortex phase-conjugating interferometer [42] is result of the usage of the $\ell = 1$ optical vortex (LG_{01}) laser beams. For the higher angular momenta of photons $\ell\hbar$ the output interference pattern have 2ℓ spots:

$$|\vec{E}|^2 = |E_{ref} + E_b|^2 \cong I(z, r, \theta, t) \sim [1 + \gamma[2L_{PCM} - 2L_{tor}] \cdot \cos[(\omega_f - \omega_b)t + 2\ell\theta]] \cdot (r/D_0)^{2|\ell|} \exp\left[-\frac{2r^2}{D_0^2(1+z^2/(k_{(f,b)}^2 D_0^4))}\right], \quad (5)$$

where z is negative provided finite optical thickness of BS is neglected (see fig.2). For the ℓ charged vortices [11] the 2ℓ spot output pattern will rotate around the common center with the angular velocity $\delta\omega/2\ell$ provided internal PCM mechanism is static and the moving internal acoustic or thermal waves are absent [9, 21, 41]. The similar interference pattern occurs in the Mach-Zehnder vortex interferometer used for excitation of the coherent vortex superpositions in quantum gases [50], slow-light media and exciton-polariton condensates [51].

Formula (5) explains 2ℓ spot output given by the overlapping of the two aligned $LG_{0\ell}$ optical vortices with parallel linear and *antiparallel* angular momenta. As in conventional Michelson interferometer the visibility of interference pattern at the output port of BS is maximal when both arms have equal optical length $L_{PCM} = L_{tor}$.

The experiments of Michelson [3] white light source have shown that constructive interference at the output port occurs even in the case when $L_{PCM}, L_{tor} \gg L_{coh}$. In our case both helical and toroidal interference patterns will also vanish in the vicinity of BS (i.e. at small *positive* z, z'). Analogously to Michelson white light interferometer the output pattern (5) will *not be affected* by finite coherence L_{coh} of the source for $L_{PCM} \sim L_{tor}$ [52].

Noteworthy the interference pattern in the nonphase-conjugating arm of interferometer located between BS and the reference mirror M is composed of the equispaced toroids separated by interval $\lambda/2$ [21]:

$$|\vec{E}|^2 = |E_f + E_{ref}|^2 \cong I(z', r, \theta, t) \sim [1 + \gamma[2(L_{tor} - z')] \cdot \cos[\delta\omega_{tor}t - (k_f + k_b)z']] \cdot (r/D_0)^{2|\ell|} \exp\left[-\frac{2r^2}{D_0^2(1 + z'^2/(k_{(f,b)}^2 D_0^4))}\right], \quad (6)$$

where L_{tor} is the length of toroidal arm, z' coordinate originating at beamsplitter BS and terminating at mirror M. The nonzero $\delta\omega_{tor}$ frequency shift is possible in this arm due to OAM tilt in reflections. For the ℓ charged vortices the pattern in toroidal arm is rotationally invariant.

IV. GEOMETRIC PHASE AND THE ANGULAR DOPPLER SHIFT ACCUMULATION

Apparently the angular momentum of photons is not changed when viewed from reference frames rotating with different angular velocities [29, 53]. But when photons pass through rotating medium the optical angular momentum changes and rotating medium experiences recoil [9, 30]. This happens due to isotropy of space [21]. Equation (7) is valid due to invariance of the Lagrangian of the system *photon plus rotating object* with respect to infinitesimal rotations $\delta\theta$. For this reason the *ideal* phase-conjugating mirror will *inevitably* modify the carrier frequency of the reflected PC photons ω_b [21] for *any* angular speed Ω_{\oplus} alike Earth rotation rate $\Omega_{\oplus} \sim 10^{-5} \text{rad/sec}$ and even smaller ones.

The elementary approach based upon conservation of energy and angular momentum demonstrated by Dholakia [49] and confirmed in other works [9] gives also the exact formula for the rotational Doppler shift induced by rotation of the PCM around propagation axis \vec{Z} :

$$\delta\omega = \omega_b - \omega_f = \pm 2\ell \Omega_{\oplus} + \frac{2\ell^2 \cdot \hbar}{I_{zz}}, \quad (7)$$

where I_{zz} is the moment of inertia of PCM with respect to \vec{Z} -axis. The second term in the right-hand size of (7) is negligible for typical masses ($m \sim g$) and sizes ($r \sim cm$) of a prisms and mirrors $\hbar/I_{zz} \sim \hbar/(m \cdot r^{-2}) \cong 10^{-27} \text{rad/sec}$. The frequency shift $\delta\omega$ is due to the inversion of the angular momentum in reflection from rotating PCM ($2\ell\hbar$) and the double passage through rotating Dove prism ($4\ell\hbar$). Using this physically transparent

arguments [9] it is easy to obtain expression for the *net* frequency shift for the photon, which passed twice, in forward and backward directions, through N image inverting elements, say Dove prisms [17] after reflection from the phase-conjugating mirror $\delta\omega_{\Sigma} = 4 \Omega_{\oplus} \ell(N + 1/2)$.

A. Invariance of the rotational frequency shift

In a *rest* (nonrotating) *frame* the conservation of energy and angular momentum is as follows :

$$\hbar\omega_f + \frac{|\vec{\mathcal{L}}_{pc}(t)|^2}{2I_{zz}} = \hbar\omega_b + \frac{|\vec{\mathcal{L}}'_{pc}(t)|^2}{2I_{zz}}, \quad \vec{\mathcal{L}}_{pc}(t) + \vec{\mathcal{L}} = \vec{\mathcal{L}}'_{pc}(t) + \vec{\mathcal{L}}', \quad (8)$$

where $\vec{\mathcal{L}}_{pc}(t)$ and $\vec{\mathcal{L}}'_{pc}(t)$ are the angular momenta of PCM and photons correspondingly before $\vec{\mathcal{L}}$ and after $\vec{\mathcal{L}}'$ photons reflection [9]. The important simplification is due to the large mass of PCM. Let us consider the tensor of inertia I_{ij} as indistinguishable from those of spherical body ($I_{zz} = I_{yy} = I_{xx}$). Then angular momentum $\vec{\mathcal{L}}$ with respect to *arbitrarily* oriented axis \vec{Z} is just $\vec{\mathcal{L}} = \vec{\Omega}_z I_{zz}$. Hence in our case (fig.2) $\vec{\mathcal{L}}_{pc} = \vec{\Omega}_{\oplus} I_{zz}$.

The slow rotation of the frame leads to the perpetual adiabatic tilt of axis $\vec{Z}(t) \parallel \vec{\mathcal{L}}_{pc} \parallel \vec{\mathcal{L}}'_{pc}$ (fig.1). Noteworthy the accurate handling with angular momentum of photons as a classical (!) vector $\vec{\mathcal{L}}$ is compatible with exact quantum picture. Let us consider the time-dependent axis of photons propagation $\vec{Z}(t)$ as a *measurement axis* [29, 53].

In quantum mechanics the projection of $\vec{\mathcal{L}}$ on a measurement axis $\vec{Z}(t)$ may have discrete values only $\mathcal{L}_z = -\ell\hbar, \dots, +\ell\hbar$. The multiplication of both sides of second equation in (8) by $\vec{\mathcal{L}}_{pc}$ yields:

$$\vec{\mathcal{L}} \cdot \vec{\mathcal{L}}_{pc}(t) + |\vec{\mathcal{L}}_{pc}(t)|^2 = \vec{\mathcal{L}}' \cdot \vec{\mathcal{L}}_{pc}(t) + \vec{\mathcal{L}}'_{pc}(t) \cdot \vec{\mathcal{L}}_{pc}(t), \quad \ell\hbar|\vec{\mathcal{L}}_{pc}| \cos\phi(t) + |\vec{\mathcal{L}}_{pc}|^2 = -\ell\hbar|\vec{\mathcal{L}}_{pc}| \cos\phi(t) + |\vec{\mathcal{L}}'_{pc}||\vec{\mathcal{L}}'_{pc}|, \quad (9)$$

where quantization of photon's angular momentum projection is included explicitly though angular momentum of *measurement device* (PCM) remains a classical vector $\vec{\mathcal{L}}_{pc}$. The second equation is due to the reversal of OAM in reflection from the PCM [21].

After some algebra with first equation in (8) and second equation in (9):

$$\ell\hbar|\vec{\mathcal{L}}_{pc}| \cos\phi(t) + |\vec{\mathcal{L}}_{pc}|^2 = -\ell\hbar|\vec{\mathcal{L}}_{pc}| \cos\phi(t) + |\vec{\mathcal{L}}'_{pc}||\vec{\mathcal{L}}'_{pc}|, \quad \hbar\omega_f + \frac{|\vec{\mathcal{L}}_{pc}|^2}{2I_{zz}} = \hbar\omega_b + \frac{|\vec{\mathcal{L}}'_{pc}|^2}{2I_{zz}}, \quad (10)$$

one may obtain the *tiny* shift of photons carrier frequency $\delta\omega$ for *noncollinear* vectors $\vec{Z}(t)$.

$\vec{\Omega}_\oplus = |\vec{\Omega}_\oplus| \cos \phi(t)$ as a result of the *stepwise* phase-conjugating OAM reversal from $\mathcal{L}_z = \pm \ell \hbar$ to $\mathcal{L}'_z = \mp \ell \hbar$:

$$\begin{aligned} \hbar \delta \omega(t) &= \frac{|\vec{\mathcal{L}}'_{pc}| - |\vec{\mathcal{L}}_{pc}|}{2I_{zz}} 2\ell \hbar \cos \phi(t) = \\ &= -2\ell \hbar |\vec{\Omega}_\oplus| \cos \phi(t) + \frac{2\ell^2 \hbar \cos^2 \phi(t)}{I_{zz}}. \end{aligned} \quad (11)$$

This $\delta \omega(t)$ shift coincides exactly with (1):

$$\delta \omega(t) = -\Delta \vec{\mathcal{L}}(t) \cdot \vec{\Omega}_\oplus / \hbar, \quad \delta \omega = -2\ell \vec{Z}(t) \cdot \vec{\Omega}_\oplus, \quad |\Delta \vec{\mathcal{L}}| = 2\ell \hbar. \quad (12)$$

Hence exchange of the angular momenta between photons and tilted rotating vortex interferometer results in angular Doppler shift affected by Coriolis multipliers ($\cos \phi(t)$ and $\cos \xi(t)$) in scalar product $\vec{Z}(t) \cdot \vec{\Omega}_\oplus$. As in the case of Foucault pendulum the 2ℓ spot interference pattern follows to the rotation of reference frame $\vec{\Omega}_\oplus$. The angle of rotation $\alpha(t)$ in a given moment t equals to the geometrical phase acquired by rotating top moving on the surface of a sphere:

$$\alpha(t) = -\int_{t_0}^t \frac{\Delta \vec{\mathcal{L}}(t) \cdot \vec{\Omega}_\oplus}{\hbar} dt = -2\ell \int_{t_0}^t \vec{Z}(t) \cdot \vec{\Omega}_\oplus dt. \quad (13)$$

In *rotating frame* the energy and angular momentum conservation for vectorial case is as follows :

$$\begin{aligned} \hbar \omega_f + 0 - \ell \hbar \Omega_\oplus &= \hbar \omega_b + \frac{|\vec{\mathcal{L}}'_{pc}(t)|^2}{2I_{zz}} + \ell \hbar \Omega_\oplus, \\ \vec{\mathcal{L}} + 0 &= \vec{\mathcal{L}}'_{pc}(t) + \vec{\mathcal{L}}', \end{aligned} \quad (14)$$

where $\mp \ell \hbar \Omega_\oplus$ is the energy transformation due to frame rotation [32]. Noteworthy the alternation of sign of this term due to reflection from PCM [21]. Again after a careful algebra the frequency shift viewed in *rotating frame* will be identical to those in *rest frame*:

$$\delta \omega(t) = -2\ell \vec{Z}(t) \cdot \vec{\Omega}_\oplus + \frac{2\ell^2 \hbar (\vec{Z}(t) \cdot \vec{\Omega}_\oplus)^2}{I_{zz}}. \quad (15)$$

B. Accumulation of rotational Doppler shift

To accumulate the rotational Doppler shift the adjacent image inverting elements (say Dove prisms) should rotate in opposite directions. This feature is due to vectorial nature of angular momentum exchange between photons and rotating Dove prisms and PCM. The following "*hand rule*" is valid due to $\delta \omega = -\Delta \vec{\mathcal{L}} \cdot \vec{\Omega}_\oplus / \hbar$: when angular momenta of photons and image inverting element are anti-parallel the energy is transferred to photon otherwise rotation of setup is accelerated at the expense of

photon [9]. For this reason the *accumulation* effect is algebraical *addition* not *multiplication*. The *accumulated* frequency shift $\delta \omega_\Sigma(z)$ is the stepwise function of z (fig.2). The smallest speed of the helix rotation $|\vec{\Omega}_\oplus| = \delta \omega / 2\ell$ is in between PCM and the first Dove prism the largest one $\delta \omega_\Sigma$ is in between the last Dove prism and beamsplitter BS.

In experimental realization the angular speeds of rotation $\vec{\Omega}_i$ of the all N image inverting elements cannot be equal to each other and some random spread of angular velocities is inevitable: $\vec{\Omega}_i = \vec{\Omega}(-1)^i + \delta \vec{\Omega}_i$. Thus generalization of $\delta \omega_\Sigma$ is required to include the random spread of the rotation frequencies $\delta \Omega_i$:

$$\delta \omega_\Sigma = -\vec{Z} \cdot (2\ell \vec{\Omega}_\oplus + 4\ell \sum_{i=1}^N \vec{\Omega}_i (-1)^i + 4\ell \sum_{i=1}^N \delta \vec{\Omega}_i), \quad (16)$$

where Ω_\oplus is the angular velocity of PC mirror.

Once PC mirror with sufficient quality is constructed the 2ℓ spot interference pattern (fig.2) will make one revolution per $86400 \cdot / (2N + 1)$ seconds with z axis oriented parallel to Earth rotation axis, e.g. in a setup located at equator and placed on a horizontal optical table.

C. Geometric phase acquired by Foucault pendulum and vortex interferometer

Coriolis force $\vec{F}_c(t) = -2M\vec{\Omega}_\oplus \times \vec{V}(t)$, where $\vec{V}(t)$ is velocity of Foucault pendulum bob in rotating frame, causes slow rotation of swinging plane with angular frequency $\Omega_{bob} = -|\vec{\Omega}_\oplus| \cos(\phi)$, where $\chi = \pi/2 - \phi$ is geographical latitude. This follows from Newtonian dynamics of the harmonic pendulum with mass M suspended in slowly rotating frame [32]. The equation of motion for the bob in rotating frame is:

$$M\vec{a} = \vec{F}_g + \vec{F}_c = -M\vec{g} - M2[\vec{\Omega}_\oplus \times \vec{V}], \quad (17)$$

where $M\vec{g}$ is the local gravity force. For the small amplitude oscillations in the (x, y) plane, where the y -axis is North directed and the x -axis is East directed at χ geographical latitude, the coupled equations for harmonic oscillations are:

$$\begin{aligned} \ddot{x} &= -\omega^2 x + 2\Omega_\oplus \cdot \dot{y} \cdot \sin \chi, \\ \ddot{y} &= -\omega^2 y - 2\Omega_\oplus \cdot \dot{x} \cdot \sin \chi, \end{aligned} \quad (18)$$

where $\omega = \sqrt{|\vec{g}|L_F} = 2\pi/T_F$ is angular frequency of bob oscillations, L_F is length of suspension wire. For complex vector $z = x + iy$ this system becomes:

$$\frac{d^2 z}{dt^2} + 2i\Omega_\oplus \cdot \frac{dz}{dt} \cdot \sin \chi + \omega^2 z = 0, \quad (19)$$

with obvious solution to the first order in Ω_\oplus/ω :

$$z = \exp[-i\Omega_{\oplus} \sin \chi t][c_1 \exp(i\omega t) + c_2 \exp(-i\omega t)], \quad (20)$$

where the arbitrary constants c_1, c_2 come from initial conditions. Noteworthy the absence of the rest mass M here. Thus swing plane of the Foucault pendulum rotates with angular velocity $\Omega_F = -\Omega_{\oplus} \sin \chi$ around local gravity acceleration vector \vec{g} . Apparently the modulus of geometrical phase $\alpha = -2\pi \sin \chi$ acquired during one rotation reaches the maximal value at the Poles (fig.1).

For the observer in a reference frame standing on the Earth the trajectory of *bob* becomes is curvilinear due to Coriolis force with the time dependent angular momentum $\vec{\mathcal{L}}_F(t)$ directed along $-\vec{g}$:

$$\vec{\mathcal{L}}_F(t) = [\vec{r} \times \vec{p}] = M[\vec{z} \times \dot{\vec{z}}], \dot{\vec{z}} + \vec{\Omega}_{\oplus} \times \vec{r} = \vec{V}. \quad (21)$$

After some algebra the angular momentum projection on $-\vec{g}$ as a function of time $\mathcal{L}_{F\text{ouc}}(t)$ might be obtained under zero velocity initial condition $\dot{\vec{z}} = 0$ for $t = 0$:

$$\begin{aligned} \mathcal{L}_F(t) = M \cdot [-2c_1c_2\Omega_{\oplus} \sin \chi \cos(2\omega t) + \\ (c_1 - c_2)(c_1 + c_2)\omega \cos(\Omega_{\oplus} \sin \chi t)^2 \cong \\ -M\Omega_{\oplus} \sin \chi \cdot 2c_1c_2 \cdot \cos(2\omega t), \quad \leftarrow \Omega_{\oplus} \ll \omega. \end{aligned} \quad (22)$$

Hence angular momentum $\mathcal{L}_F(t)$ oscillates with period $\pi/\omega = T_F/2$.

In Michelson vortex interferometer (fig.2) the photons with zero rest mass and the angular momentum $\mathcal{L}_Z = \pm \ell \hbar$ are also affected by frame rotation when their angular momentum direction is changed via phase conjugation and passage through Dove prisms [9]. The optomechanics of this *spin-orbital* interaction is a δ -kicked one: the most of the time the photons with angular momentum $\mathcal{L}_z = \pm \ell \hbar$ moves in free space. At the moments separated by time of flight intervals $2\Delta L_{pc}/c$ the δ -kicks adjust the helical phase front $\exp(i\ell\theta)$ to the gradually changing orientation of interference pattern inside PCM.

The reversal of the photons angular momentum in rotating PCM and Dove prism might be interpreted as effective "Coriolis" force induced by a slowly moving fringes of interference pattern in PCM and tilted planes in Dove prism. This leads to rotation of the helical interference pattern [9] with the the similar angular velocity $\Omega_{pc} = \delta\omega/2\ell = -|\vec{\Omega}_{\oplus}| \cos \phi = \Omega_F$ as it happens with Foucault pendulum.

In both cases the initial conditions are essential. In PCVI (fig.2) the interference fringes inside PCM and vortex fringes must be adjusted when holographic plate is used as PCM, while Foucault pendulum *bob* ought to be gently released from maximal deflection point with zero initial velocity $\dot{\vec{z}} = 0$. Then *bob* begins to fall towards equilibrium position but its trajectory gradually bends because of Coriolis force which is the source of the periodically modulated angular momentum $\vec{\mathcal{L}}_F(t)$ [1].

D. The mutual orientation of the setup rotation axis $\vec{\Omega}_{\oplus}$ and vortex propagation axes \vec{Z} and \vec{Z}'

Consider the important issue which stems from the angular momentum transformation in PCVI. Noteworthy the case when axis of rotation $\vec{\Omega}_{\oplus}$ and *toroidal* axis \vec{Z}' are mutually orthogonal the net angular Doppler shift is absent ($\delta\omega = 0$). In this case backward wave in *toroidal* arm acquires the additional Doppler shift $\delta\omega_{tor} = \ell \Omega_{\oplus}$ due to angular momentum tilt at 90° in BS after backward reflection from BS. This case is the worst suited for usage as reference wave to observe the beats (5) with angular frequency $\delta\omega$ due to superposition with backward wave from *helical* arm. For orthogonal helical and toroidal arms the rotational Doppler shift between waves in the output port is exactly zero. This follows from *hand rule* used for analysis of OAM transformation in passage through BS, PCM and reflection from M. The best mutual orientation of \vec{Z} and \vec{Z}' is to be almost parallel ($\eta \rightarrow 0$) in order to minimize the OAM change via deflection inside BS because the later rotates together with setup. For this reason the different tuning angles are selected at (fig.2): ϕ is the angle between rotation axis $\vec{\Omega}_{\oplus}$ (say targeted to Polar star) and helical (PCM) axis, while η is angle between \vec{Z} and \vec{Z}' (6).

V. VORTEX MICHELSON INTERFEROMETER AND THE LASER NOISE

A. Phase noise and visibility of helical pattern

The fundamental limit on the laser phase noise is given by the Shawlov-Townes formula [34] which connects the laser linewidth $\delta\nu_{ST}$ with emitted power P , cavity mode bandwidth $\Delta\nu_c$ and effective temperature of the lasing medium T_L :

$$\delta\nu_{ST} \sim 4\pi(\hbar\omega_{f,b} + k_B T_L)(\Delta\nu)^2/P. \quad (23)$$

The amplitude fluctuations are assumed to form background of the narrow stimulated emission line $\delta\nu_{ST}$ which is due to the phase fluctuations diffusion with characteristic coherence time τ_c .

In order to generalize the previous analysis [19] for visibility of patterns in PC vortex interferometer [21, 42] (fig.1), let us take for definiteness the electric field envelopes in the form of Laguerre-Gaussian beam (LG) [21]:

$$\begin{aligned} E_{(f,b)}(\vec{r}, t) \sim \frac{\exp[-i\omega_{(f,b)}t \pm ik_{(f,b)}z \pm i\ell\theta + i\Theta_{(f,b)}(t)]}{(1+iz/z_R)} \\ E_{(f,b)}^0(r/D_0)^{|\ell|} \exp[-\frac{r^2}{D_0^2(1+iz/z_R)}], z_R = k_{(f,b)}D_0^2 \end{aligned} \quad (24)$$

or a Bessel beam optical vortex [48]:

$$\begin{aligned} \mathbf{E}_{(\mathbf{f},\mathbf{b})}(\vec{\mathbf{r}}, \mathbf{t}) \sim E_{(f,b)}^0 \cdot J_m(\kappa r) \\ \exp[-i\omega_{(f,b)}t \pm ik_{(f,b)}z \pm i\ell\theta + i\Theta_{(f,b)}(t)], \end{aligned} \quad (25)$$

where the cylindrical coordinates $\vec{r} = (z, r, \theta)$ are used, \mathbf{E}_f stands for the forward wave (fig.1), propagating in positive Z-direction, \mathbf{E}_b stands for the wave, propagating in the opposite direction, $J_m(\kappa r)$ is the m-th order Bessel function, $\Theta_{(f,b)}(t)$ are the random variations of the phases of partial waves, induced by both the laser linewidth and fluctuations inside interferometer [54].

The interference pattern produced by two vortices with phase noise $\Theta_f(t)$ and $\Theta_b(t)$ is as follows:

$$|\vec{E}|^2 = |E_f + E_b|^2 \cong I(z, r, \theta, t) \sim [1 + [\cos(\omega_f - \omega_b)t - (k_f + k_b)z + 2\ell\theta + \Theta_f(t) - \Theta_b(t)]] \cdot (r/D_0)^{2|\ell|} \exp\left[-\frac{2r^2}{D_0^2(1 + z^2/(k_{(f,b)}^2 D_0^4))}\right], \quad (26)$$

The pattern breaths due to slow random drift of phases $\Theta_f(t)$ and $\Theta_b(t)$. Taking into account that counterpropagating vortices are produced via reflection from PCM, i.e. $\Theta_f(t) = \Theta(t+T) = \Theta_b(t-T)$ where $T = 2(L_{PCM} - z)/c$ is time delay at a given point z on interferometer axis, we have for statistically averaged interference pattern at output port (fig.2):

$$\overline{|E_f + E_b|^2} \sim \left\{1 + \left[1 - \frac{(\Theta(t) - \Theta(t-T))^2}{2!}\right] \cdot \cos[(\omega_f - \omega_b)t - (k_f + k_b)z + 2\ell\theta]\right\} \cdot (r/D_0)^{2|\ell|} \exp\left[-\frac{2r^2}{D_0^2(1 + z^2/(k_{(f,b)}^2 D_0^4))}\right], \quad (27)$$

with apparent averaging of the first term $(\Theta(t) - \Theta(t-T)) = 0$ of this Taylor expansion justified for narrow linewidth $\delta\nu_{ST}$. The second order correlation function γ or visibility of pattern is as follows:

$$\gamma[2(L_{PCM} - z)] = 1 - \frac{(\Theta(t) - \Theta(t-T))^2}{2!}, \quad (28)$$

with apparent limit $\gamma \rightarrow 1$ as $T \rightarrow 0$.

B. Quantum state transformation in the ideal vortex phase-conjugator

Generally speaking statistics of the phase-conjugated photons [55] changes due to the mixing with amplified vacuum modes[56] incident from open rear ports of PCM [35]. However there exists an example of the PCM that does not change statistics of PC-reflected photons. Indeed the Sagnac loop PCM proposed in [41] (fig.3) may operate without coupling of incident signal with external modes in the case of negligible absorption and amplification inside PCM. This happens in a quite realistic case of the perfect 50/50 beamsplitter when each incident vortex photon in an *arbitrary* quantum state $|q\rangle$ moves along two paths (clockwise and counterclockwise) with identical optical lengths L_+ and L_- . The same happens

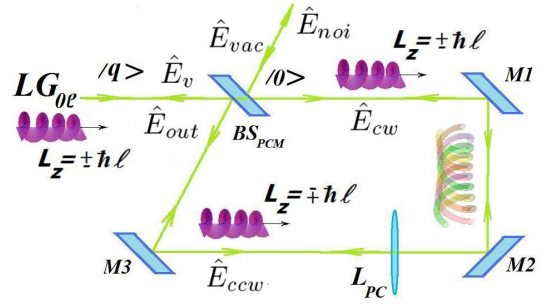


FIG. 3: (Color online) Ideal PCM for isolated vortex photons. BS_{PCM} is entrance beamsplitter of PCM, M_{1-3} are conventional mirrors, L_{PC} is wavefront matching lens, $|0\rangle$ is vector of state of vacuum, $|q\rangle$ is a vector of state of vortex photon emitted by laser.

with the vacuum modes $|0\rangle$ incident through the open port of BS_{PCM} and recombining after propagation along the equal paths L_+ and L_- . In Heisenberg picture the interference pattern inside PCM looks as follows:

$$\begin{aligned} \hat{E}_{ccw} &= \sqrt{R_{in}} \hat{E}_v + \sqrt{T_{in}} \hat{E}_{vac}, \\ \hat{E}_{cw} &= \sqrt{T_{in}} \hat{E}_v - \sqrt{R_{in}} \hat{E}_{vac}, \end{aligned} \quad (29)$$

where \hat{E}_v is the incident vortex field, \hat{E}_{vac} is the vacuum zero-point field, \hat{E}_{cw} is clockwise field inside the PCM, \hat{E}_{ccw} is counterclockwise field inside the PCM, R_{in} and T_{in} are intensity reflectance and transmittance of the entrance beamsplitter BS_{PCM} of PCM. Then output annihilation (electric field) operators \hat{E}_{out} and \hat{E}_{noi} are:

$$\begin{aligned} \hat{E}_{out} &= \sqrt{T_{in}} \hat{E}_{ccw} + \sqrt{R_{in}} \hat{E}_{cw}, \\ \hat{E}_{noi} &= \sqrt{T_{in}} \hat{E}_{cw} - \sqrt{R_{in}} \hat{E}_{ccw}, \end{aligned} \quad (30)$$

or in the terms of the input fields operators:

$$\begin{aligned} \hat{E}_{out} &= 2\sqrt{T_{in}R_{in}} \hat{E}_v + (T_{in} - R_{in}) \hat{E}_{vac}, \\ \hat{E}_{noi} &= -2\sqrt{T_{in}R_{in}} \hat{E}_{vac} + (T_{in} - R_{in}) \hat{E}_v. \end{aligned} \quad (31)$$

Thus for peculiar case $T_{in} = R_{in} = 1/2$ the noise contribution in the output field \hat{E}_{out} is completely suppressed and the incident vortex photons return via constructive interference at BS_{PCM} in exactly opposite direction with inverted momentum $-\vec{k}$ and opposite angular momentum $-\vec{L}$. As a result the all zero-point noise incident through the open rear port BS_{PCM} is removed via constructive interference at BS_{PCM} .

The composite quantum state of the vortex photons and vacuum fluctuations $|\psi\rangle = |q\rangle |0\rangle$ remains unperturbed in Heisenberg picture. Moreover for $T_{in} = R_{in} = 1/2$ the statistics is not changed. The wavefront matching lens L_{PC} located at the midway of the loop

(fig.3) compensates the natural beam divergence of vortex and external vacuum fields. This remove the mixing with another propagation modes different from incident vortex.

The vortex linewidth may be evaluated as coherent state CS whose linewidth $\delta\nu_{CS} \lesssim \delta\nu_{ST}$ approximately corresponds to uncertainty relation for number of photons n and phase ϕ [57]:

$$\delta n \cdot \delta\phi \sim 1; \delta\phi = \frac{1}{\delta n} = \frac{1}{\sqrt{n}} = \sqrt{\frac{\hbar\omega_{(f,b)}}{\epsilon_0 VI}}, \quad (32)$$

where ϵ_0 is free space permittivity, V is mode volume, $I \cong |E_{(f,b)}|^2$ is light intensity. One may suggest that a higher density of the interference fringes (2ℓ per $\lambda/2$) in helical interference pattern may enhance the phase sensitivity of Michelson interferometer by a factor $(2\ell)^\alpha$ [36], where $1 \leq \alpha \leq 2$:

$$(2\ell)^\alpha \delta n \cdot \delta\phi \sim 1; \delta\phi = \frac{1}{(2\ell)^\alpha \sqrt{n}} = \sqrt{\frac{\hbar\omega_{(f,b)}}{\epsilon_0 VI (2\ell)^{2\alpha}}}. \quad (33)$$

Furthermore in a structured squeezed state limit [58, 59] the ultimate resolution may reach even the smaller values:

$$(2\ell)^\alpha \delta n \cdot \delta\phi \sim 1; \delta\phi = \frac{1}{\delta n} = \frac{1}{n} = (2\ell)^{-\alpha} \frac{\hbar\omega_{(f,b)}}{\epsilon_0 VI}. \quad (34)$$

Such a significant reduction of the phase uncertainty requires the accurate quantum measurements procedures [60]. In this way the sensitivity of Michelson interferometer to coarse displacements might be improved by $3 \div 4$ orders of magnitude using currently achievable vortex laser beams with topological charges $\ell \sim 10^3 \div 10^4$ [61]. The underlying idea is that the structured interference pattern with 2ℓ spots behind output beamsplitter (fig.2) will rotate faster when ℓ is increased. Though the phase fluctuations of the laser beam could mask the external perturbations of space-time metric (optical path difference in fig.2) the coarse azimuthal interference pattern structured by the 2ℓ factor would facilitate the detection of tiny changes of optical paths. This conjecture requires the detailed quantitative study with the quantum measurements theory[5].

VI. CONCLUSIONS

In summary the Michelson phase-conjugating vortex interferometer (fig.2) had been analyzed for the purpose of detection of the ultraslow rotations and tiny metric disturbances using concept of an *ideal* PCM [41] and a fact that optical vortex propagation in free space is not affected by a choice of reference frame [9, 30]. The novel

feature compared to [21] which is close to Beth's *spin* of photon *phase – conjugating* torsion pendulum experiment [33] is in the additional reference arm where the nonrotating vortex beam is stored [42] (fig.2). This gives the robustness of the interferometer and possibility to use the broadband light source with $L_{coh} > |L_{PCM} - L_{tor}|$ in contrast to previous studies [9, 21] where $L_{coh} > L_{PCM}$ is the necessary condition for the visible interference pattern. The motion of the circular interference fringes due to changes of the optical paths difference resembles the operation of the Foucault pendulum [1] where bob marks the points on the circle corresponding to a given rotation angle of reference frame.

The actual range of detectable frequencies of the slow rotations might be augmented by a set of image-inverting counter-rotating elements N in PCM arm of PCVI. The accumulated angular Doppler shift grows linearly with N . The explicit expression have been obtained for $\delta\omega_{net}$ including the random spread of rotation velocities Ω_i .

In simplest configuration, i.e. without accumulating Dove prisms with oppositely directed angular velocities $\vec{\Omega}_i$, the proposed vortex interferometer will contain no rotating parts or lasers with unique features. The propagation of vortex beams follows here to the conventional transformation optics [67].

As a well known Beth setup for the optical torque measurement [33] and Mach-Zehnder vortex interferometer for the rotational Doppler effect demonstration [49] the our proposal (fig.2) is based entirely on the Maxwell equations and Einstein relativity without usage of any additional assumptions alike "ether theory".

The ultimate performance of the Michelson vortex interferometer is limited by the quantum noise of laser as in conventional Michelson interferometer [56]. Hopefully there exists opportunity to improve the sensitivity by a factor $(2\ell)^\alpha$ with the aid of the azimuthally structured interference pattern of topologically charged laser beams [21, 42]. The further increase of the sensitivity looks promising with the superfluid interferometry in lattices [62], helical traps [63–66] and exciton-polariton condensates [51].

The mechanism of detection is the *dragging* of 2ℓ spot interference pattern formed by interference fringes within PCM. In this minimal configuration vortex interferometer is the optomechanical proof of the isotropy of space. From the point of view of observer collocated with interferometer in the slowly rotating frame the 2ℓ spot pattern circumvents around the LG beam axis. To this rotating observer the vortex beam reflected from the PCM acquires the angular Doppler shift $\delta\omega$. On the other hand from the point of view of observer placed on "remote unmovable star" (i.e. *rest frame*) the anisotropic PC mirror *drags* the twisted interference pattern.

VII. DISCLOSURES

Author declare no conflicts of interest.

-
- [1] L.Foucault, "Démonstration physique du mouvent de rotation de la Terre, au moyen d'un pendule", Comptes rendus hebdomadaires des seances de l'Academie des Sciences (Paris), vol. 32, p.135-138 (1851).
- [2] M.Born and E.Wolf, "*Principles of Optics*", Cambridge University Press, Cambridge(1972).
- [3] A.A.Michelson, "Relative Motion of Earth and Aether", Philosophical Magazine v.8 (48), 716-719 (1904).
- [4] G. Sagnac, "On the proof of the reality of the luminiferous aether by the experiment with a rotating interferometer", Comptes Rendus, vol.157, p. 1410-1413 (1913).
- [5] M.O.Scully, M.S.Zubairy, "*Quantum optics*", Ch.4, (Cambridge University Press) (1997).
- [6] B.P. Abbott et al., "Observation of Gravitational Waves from a Binary Black Hole Merger", Phys.Rev.Lett., **116**, 061102 (2016).
- [7] M. E. Gertsenshtein, V. I. Pustovoit, "On the detection of low frequency gravitational waves", JETP, **16(2)**, 433(1963).
- [8] B.P.Abbott et al., "LIGO: the Laser Interferometer Gravitational-Wave Observatory", Rep. Prog. Phys.,**72(7)**, 076901 (2009).
- [9] A.Yu.Okulov, "Rotational Doppler shift of the phase-conjugated photons", J. Opt. Soc. Am. B **29**, 714-718 (2012).
- [10] J.F.Nye and M.V.Berry, "Dislocations in wave trains," Proc.R.Soc.London, Ser.A, **336**,165(1974).
- [11] L.Allen, M.W.Beijersbergen, R.J.C.Spreeuw and J.P.Woerdman, "Orbital angular momentum of light and the transformation of Laguerre-Gaussian laser modes," Phys.Rev.A, **45**,8185-8189 (1992).
- [12] J.Leach,M.J.Padgett,S.M.Barnett,S.Franke-Arnold, and J.Courtial, "Measuring the Orbital Angular Momentum of a Single Photon", Phys.Rev.Lett. **88**, 257901 (2002).
- [13] Yongxiong Ren, Guodong Xie, Hao Huang, Nisar Ahmed, Yan Yan, Long Li, Changjing Bao, Martin P. J. Lavery, Moshe Tur, Mark A. Neifeld, Robert W. Boyd, Jeffrey H. Shapiro, and Alan E. Willner, "Adaptive-optics-based simultaneous pre- and post-turbulence compensation of multiple orbital-angular-momentum beams in a bidirectional free-space optical link", Optica,**1(6)**,376-382 (2014).
- [14] M. V. Vasnetsov,I. G. Marienko, M. S. Soskin, "Self-reconstruction of an optical vortex", JETP Lett., **71**, 130-133 (2000).
- [15] G. Gbur, R.K. Tyson, "Vortex beam propagation through atmospheric turbulence and topological charge conservation", Journ.Opt.Soc.Am. A, **25**, 225-230 (2008).
- [16] M.R.Dennis, R.P.King, B.Jack, K.O'Holleran, and M.J.Padgett, "Isolated optical vortex knots", Nature.Phys.,**6**, 118(2009).
- [17] A. Bekshaev, M.Soskin and M. Vasnetsov, "Paraxial Light Beams with Angular Momentum" Nova Science(2008).
- [18] G.Gbur, "*Singular Optics*", CRC Press (2016).
- [19] J. Arlt, M. MacDonald, L. Paterson, W. Sibbett, K. Volke-Sepulveda and K. Dholakia, Opt. Express, **10** (19), 844 (2002).
- [20] N.G.Basov, I.G.Zubarev,A.B.Mironov, S.I.Mikhailov and A.Y.Okulov, "Laser interferometer with wavefront reversing mirrors", JETP, **52**, 847(1980).
- [21] A.Yu.Okulov,"Angular momentum of photons and phase conjugation", J.Phys.B., **41**, 101001 (2008).
- [22] P.Senthilkumaran, B.Culshaw and G.Thursby, "Fiber optic Sagnac interferometer for the observation of Berry's topological phase", J. Opt.Soc.Am. B, **17**, 1914-1919 (2000).
- [23] P.Senthilkumaran, G.Thursby and B.Culshaw, "Fiber-optic tunable loop mirror using Berry's geometric phase", Opt.Lett., **25**, 533-535 (2000).
- [24] Ruchi B.S., Bhargava Ram, and P.Senthilkumaran, "Hopping induced inversions and Pancharatnam excursions of C-points", Opt.Lett., **42**, 4159-4162 (2017).
- [25] A. Tomita and R. Y. Chiao, "Observation of Berry's topological phase by use of an optical fiber", Phys. Rev. Lett., **57**, 937-940 (1986).
- [26] M. V. Berry, "Interpreting the anholonomy of coiled light", Nature,**326**, 277-278 (1987).
- [27] J.F.Nye and M.V.Berry, "Quantal phase factors accompanying adiabatic changes," Proc.R.Soc.London, Ser.A, **392**,45-57(1984).
- [28] S. Pancharatnam, "Generalized theory of interference, and its applications," Proc.Indian Acad.Sci.,Sect. A, **44**,247-262(1956).
- [29] E.M.Lifshitz, L.P.Pitaevskii and V.B.Berestetskii, "*Quantum Electrodynamics*", (Oxford:Butterworth-Heinemann) (1982).
- [30] F.C. Speirits, M.P.J. Lavery, M.J. Padgett, S.M. Barnett, "Optical Angular Momentum in a Rotating Frame", Opt. Lett.,**39(10)**, 2944-2946 (2014).
- [31] K. Y. Bliokh, Y. Gorodetski, V.Kleiner, and E. Hasman, "Coriolis Effect in Optics: Unified Geometric Phase and Spin-Hall Effect" Phys.Rev.Lett., **101**, 030404 (2008).
- [32] L.D. Landau and E.M. Lifshitz, "*Mechanics*", Butterworth-Heinemann, Oxford (1976).
- [33] R.A. Beth,"Mechanical detection and measurement of the angular momentum of light," Phys.Rev., **50**, 115(1936).
- [34] A. L. Schawlow and C. H. Townes, "Infrared and optical masers", Phys. Rev. **112**, 1940 (1958).
- [35] A.L.Gaeta, R.W.Boyd,"Quantum noise in phase-conjugation", Phys.Rev.Lett., **60**, 2618(1988).
- [36] L.A.Lugiato, Ph.Grangier, "Improving quantum-noise reduction with spatially multimode squeezed light",J. Opt.Soc.Am. B, **14**, 225-231 (1997).
- [37] B.Y.Zeldovich, N.F.Pilipetsky and V.V.Shkunov, "*Principles of Phase Conjugation*", (Berlin:Springer-Verlag)(1985).
- [38] A.V.Mamaev, M.Saffman and A.A.Zozulya, "Time dependent evolution of an optical vortex in photorefractive media", Phys.Rev.A, **56**, R1713 (1997).
- [39] P.V.Polyansky and K.V.Felde, "Static Holographic Phase Conjugation of Vortex Beams", Optics and Spectroscopy, **98**, 913-918 (2005).
- [40] D.V.Petrov and J.W.R.Tabosa,"Optical Pumping of Orbital Angular Momentum of Light in Cold Cesium Atoms", Phys.Rev.Lett., **83**,4967(1999).
- [41] A.Yu.Okulov, "Phase-conjugation of the isolated optical vortex using a flat surfaces", J. Opt. Soc. Am. B, **27**, 2424-2427 (2010).
- [42] M.Woerdemann, C.Alpmann and C.Denz,"Self-pumped

- phase conjugation of light beams carrying orbital angular momentum", *Opt. Express*, **17**, 22791(2009).
- [43] Courtial J., Robertson D. A., Dholakia K., Allen L. and Padgett M. J., "Measurement of the Rotational Frequency Shift Imparted to a Rotating Light Beam Possessing Orbital Angular Momentum", *Phys.Rev.Lett.*, **81**,4828(1998).
- [44] A.Yu.Okulov, "Twisted speckle entities inside wavefront reversal mirrors", *Phys.Rev.A* , **80**, 013837 (2009).
- [45] E.G. Abramochkin and V.G. Volostnikov, "Relationship between two-dimensional intensity and phase in a Fresnel diffraction zone", *Opt.Comm.*, **74**, p.144 (1989).
- [46] A.Yu.Okulov, "Optical and Sound Helical structures in a Mandelstam - Brillouin mirror", *JETP Lett.*, **88**, 631 (2008).
- [47] M.Woerdemann, "*Structured Light Fields*", (Springer) (2012).
- [48] K.Volke-Sepulveda and R.Jauregui, "All-optical 3D atomic loops generated with Bessel light fields," *J.Phys.B.*, **42**, 085303 (2009).
- [49] M. P. MacDonald, K. Volke-Sepulveda, L. Paterson, J. Arlt, W. Sibbett and K. Dholakia. "Revolving interference patterns for the rotation of optically trapped particles", *Opt.Comm.*,**201**(1-3),21-28 (2002).
- [50] K. T. Kapale , J. P. Dowling, "Vortex Phase Qubit: Generating Arbitrary, Counterrotating, Coherent Superpositions in Bose-Einstein Condensates via Optical Angular Momentum Beams",*Phys.Rev.Lett.*, **95**, 173601 (2005).
- [51] F.I. Moxley III, Weizhong Dai, J. P. Dowling, T.Birnes, "Sagnac interferometry with coherent vortex superposition states in exciton-polariton condensates",*Phys.Rev.A*, **93**, 053603 (2016).
- [52] S. M. Rytov, Yu. A. Kravtsov and V. I. Tatarskii, "*Principles of Statistical Radiophysics*", (Kluwer Academic Publishers), (1987).
- [53] A.I.Akhiezer and V.B.Berestetskii, "*Quantum Electrodynamics*", (Interscience Publishers)(1965).
- [54] A.E.Siegman, "*Lasers*", (Oxford) (1986).
- [55] I.G.Zubarev, A.B.Mironov, S.I.Mikhailov and A.Yu.Okulov, "Accuracy of reproduction of time structure of the exciting radiation in stimulated scattering of light", *JETP*, **57**, 270 (1983).
- [56] Carlton M. Caves, "Quantum-mechanical noise in an interferometer", *Phys.Rev.D*, **23**, 1693(1981).
- [57] J.P. Dowling,"Correlated input-port, matter-wave interferometer: quantum-noise limits to the atom-laser gyroscope", *Phys.Rev.A*, **57**, 4736(1998).
- [58] J.P. Dowling, "Quantum optical metrology-the lowdown on high-N00N states", *Contemporary Physics*, **49**(2), 125(2008).
- [59] L. A. Lugiato and F. Castelli,"Quantum Noise Reduction in a Spatial Dissipative Structure", *Phys.Rev.Lett.*, **68**(22), 3284-3286(1992).
- [60] H. A. Haus and Y. Yamamoto, "Preparation, measurement and information capacity of optical quantum states", *Rev. Mod. Phys.*, **58**, 1001 (1986).
- [61] M.J.Padgett, F.M.Miatto, M.P.J.Lavery, A.Zeilinger, R.W.Boyd, "Divergence of an orbital-angular-momentum-carrying beam under propagation", *New.Journ.Phys*, **17**(2), 023011 (2015).
- [62] Jesus Cuevas, Boris A. Malomed, and P. G. Kevrekidis Two-dimensional discrete solitons in rotating lattices. *Phys.Rev.E* 2007; **76**, 046608.
- [63] A.Yu.Okulov, "Cold matter trapping via slowly rotating helical potential", *Phys.Lett.A*, **376**, 650-655 (2012).
- [64] A.Yu.Okulov, "Superfluid rotation sensor with helical laser trap", *Journ.Low.Temp.Phys.*, **171**, 397-407 (2013).
- [65] A. Al Rsheed, A. Lyras, O. M. Aldossary and V. E. Lembessis, "Rotating optical tubes for vertical transport of atoms", *Phys.Rev.A* , **94**, 063423 (2016).
- [66] V. E. Lembessis , A.Alqarni,S.Alshamari, A.Siddig, O. M. Aldossary "Artificial gauge magnetic fields and electric fields for free two-level atoms interacting with optical Ferris wheel light fields" , *J. Opt. Soc. Am. B*. **34**, 1122-1129(2017).
- [67] G. Gbur and O.Korotkova, "Orbital angular momentum transformations by non-local linear systems", *Opt.Lett.*, **47**, 321-324 (2022).<https://doi.org/10.1364/OL.447434>